The Fluid Mechanics of Pulsed Laser Propulsion

Girard A. Simons* and Anthony N. Pirri*
Physical Sciences Inc., Woburn, Mass.

A fluid mechanical model is developed to assess the performance of a rocket that is propelled by the absorption of radiant energy from a remotely stationed, repetitively pulsed laser. The model describes the flow within a conical nozzle that is subjected to point energy depositions at the apex of the cone. A similarity solution is obtained and the specific impulse and energy efficiencies that may be achieved with such a device are determined. Fluid mechanical constraints limit the range of pulse repetition rates that may be utilized. Preliminary design considerations indicate that a specific impulse of 800 sec or greater may be achieved with both a laboratory and a full-scale device. A two pound laboratory rocket can be accelerated at 10 *g*'s with a 15 joule laser pulsed 25,000 times per sec. A one ton rocket will require a megajoule laser operating at 350 pulses per sec to achieve an equivalent acceleration.

Nomenclature

A,a = constants in shock motion [Eq. (4)]
D^* = nozzle throat diameter
dm = mass element
e_R = relative efficiency [Eq. (22)]
E = laser energy per pulse
$F(\theta_c)$ = thrust reduction in flow divergence [Eq. (17)]
$f(\eta)$ = dimensionless density
$g(\eta)$ = dimensionless pressure
g = acceleration of gravity
$h(\eta)$ = dimensionless velocity
I_1,I_2,I_3 = integrals over similarity solution
I_{sp} = specific impulse
L = nozzle length
M = mass released per pulse
$\dot{M}$ = instantaneous source mass flux
P = instantaneous power
p = gas pressure
Q_∞ = dimensionless exhaust pressure
r = spherical radius
R_s = spherical radius of shock
T = instantaneous thrust or gas temperature where indicated
t = time
t_c = maximum time between pulses (Fig. 5a)
t_{max} = limit of strong shock solution (Fig. 5a)
t_p = time between pulses (Fig. 5b)
t_b = shock breakthrough time (Fig. 5b)
t_s = source delay time
u = fluid velocity
u_l = limiting gas velocity
V_s = shock velocity
γ = c_p/c_v
η = similarity coordinate $r/R_s(t)$
θ_C = cone half angle
ρ = gas density
τ = dimensionless time between pulses
Ω = solid angle of conical nozzle

Subscripts

l = conditions upstream of shock
b = breakthrough conditions
e = exit plane conditions
s = shock and post shock conditions
∞ = ambient conditions

Superscripts

$*$ = sonic conditions
$-$ = time or mass average

Received Oct. 19, 1976; revision received March 16, 1977.
Index categories: Nonsteady Aerodynamics; Shock Waves and Detonations; Lasers.
*Principal Scientist. Member AIAA.

I. Introduction

In recent years, several authors[1-7] have discussed and analyzed the possibility of using beamed laser energy for rocket propulsion, often with specific reference to the application of high power, ground based lasers. The concept is deceptively simple: provide a high energy density for propulsion without the encumbrance of a massive onboard power supply. Radiation from a remotely stationed high power laser is focused onto an absorbing propellant and a high temperature plasma is created. The specific impulse resulting from these energy densities can be significantly greater than those obtained for chemical rockets and the ratio of payload to vehicle weight may be greatly increased.

A series of experiments to determine the specific impulse and the thrust to laser power that can be obtained with existing laser systems is described in Ref. 4. Steady-state simulation experiments were performed in a vacuum chamber with solid propellants. A steady-state or CW (continuous working) laser propulsion system is a system whose thrust remains constant in time while the laser beam continuously provides the energy to the propellant. It was found that a high ratio of thrust to laser power can be obtained by simply using the laser to vaporize a solid surface. However, in order to obtain high specific impulse, it is necessary to add energy to the vapor. The vapor is a weakly ionized gas. The heating of this vapor by the absorption of radiation via inverse Bremsstrahlung was found to be inherently unstable. The stability of laser heated flows both upstream and downstream of a nozzle throat is not adequately understood and is a very complex issue.[7] However, it appears that stable heating of a propellant in a steady-state manner may best be accomplished by heating the gas upstream of a throat such that the beam direction and the propellant flow direction are the same. This would require a laser window in the absorption chamber that will tolerate transmission of significant laser intensities along with high pressures for long periods of time.

The alternative approach to laser propulsion that circumvents the stability problem is to utilize a pulsed laser.[4] The techniques for obtaining large thrust and specific impulse with a pulsed laser are an outgrowth of various experimental and theoretical programs in laser effects.[8-12] When a high power pulsed laser is focused to a high intensity in a gas or on a solid surface, a high temperature, high pressure plasma is initiated which propagates up the laser beam. If the duration of the laser pulse is sufficiently short that the high pressure

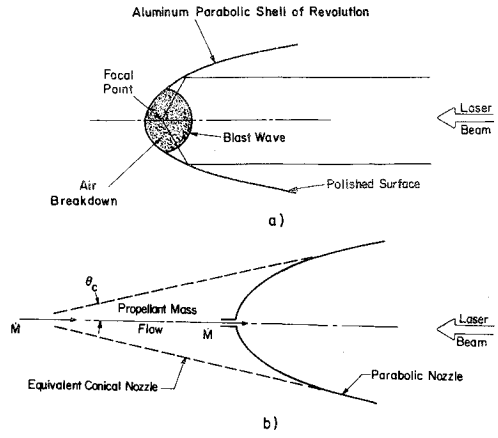

Fig. 1 a) Single pulse propulsion concept as introduced in Ref. 4; b) multiple pulse propulsion concept and equivalent conical nozzle.

gas remains in the vicinity of a surface or nozzle wall during the energy deposition, this method may be an efficient propulsion mechanism. The propulsion system operates in a way similar to detonation propulsion systems that have been proposed for use in high pressure environments.[13] Periodic "explosions" in the nozzle transfer the detonation or laser energy to the working fluid. The two most significant potential advantages afforded by a pulsed laser propulsion system over a CW laser propulsion system are 1) simplicity in engine design as a result of permitting the laser beam to enter the nozzle via the exhaust plane, and 2) elimination of constraints resulting from plasma instability. However, the power conversion efficiency (efficiency of converting laser power to power in the rocket exhaust) must be determined. In the early experiments[4] on pulsed laser propulsion, the power conversion efficiency was only a few percent because the laser pulse duration was too long. For an infinitely short pulse duration such as that considered here, thrust is obtained by converting laser energy to propellant kinetic energy via a continuously weakening shock wave. It is not known, a priori, if the efficiency of generating thrust in this manner is the same as when converting laser power to thrust in a steady process.

The purpose of the present study is to provide a detailed study of the fluid mechanics of pulsed laser propulsion. The objective is to determine the relative efficiency of a pulsed laser propulsion system compared to a CW system and to calculate the specific impulse and thrust as a function of laser power, pulse repetition frequency, ambient conditions and propellant mass flow. The nozzle configuration is taken to be an idealized extension of the concept introduced in Refs. 2 and 4. A schematic of the single pulse nozzle configuration[2,4] is presented in Fig. 1a. The nozzle walls focus the incoming beam to yield a breakdown in the air at the focal point. For a sufficiently short pulse duration, a blast wave forms and propagates to the nozzle exit plane. The high pressure gas behind the shock provides the force on the nozzle wall. The nozzle was designed for single pulse operation only. Therefore, no considerations of propellant supply were necessary. In this study, the fluid mechanics of a repetitively pulsed laser propulsion system is analyzed, and thus, the fluid dynamics of the propellant feed system is included. The configuration to be analyzed is shown in Fig. 1b. The nozzle drawn with a solid line is the parabolic self-focusing nozzle. However, for simplicity, this nozzle is replaced by a conical nozzle which is shown dashed in the figure. The angle of the cone is chosen such that the exhaust gases leave the exit plane at the same angle relative to the thrust axis as with the parabolic nozzle. The beam is assumed to be focused externally such that the focusing angle equals the cone angle. The propellant is treated as a steady source flow entering the apex or "throat" of the conical nozzle. Periodically, laser induced blast waves are ignited at $r=0$ where r is measured from the apex. In the following sections, a theory is developed to describe a single pulse, and then extended to multiple pulses in order to determine the specific impulse and thrust as a function of pulse repetition frequency. A discussion of operational limitations such as the effects of the cone angle, nozzle length and finite exit plane pressure are also included.

II. Single Pulse Theory

Consider the steady flow of a propellant through a conical nozzle of solid angle Ω. The gas flow is, by assumption, spherically symmetric, isentropic and constant γ. The gas velocity in the supersonic portion of the nozzle is assumed to reach the limiting velocity of the gas at zero temperature;

$$u_l = u_\ell = \left(\frac{\gamma+1}{\gamma-1}\right)^{1/2} u^* \tag{1}$$

where u^* is the sonic gas velocity. The corresponding gas density ρ_l is expressed as

$$\rho_l = \rho^*(r^*)^2 \Big/ \left(\frac{\gamma+1}{\gamma-1}\right)^{1/2} r^2 \tag{2}$$

where ρ^* is the density at sonic conditions, r is the spherical radius and r^* is the radius of the hypothetical "source" of strength $\dot{M}$,

$$\dot{M} = \rho^* u^* (r^*)^2 \Omega$$

Equations (1) and (2) represent the gas velocity and density downstream of the source radius r^*. There is a local failure of the equations for $r \leq 0$ (r^*). However, mass flux is conserved within this radius.

At $t=0$ we shall (with a pulsed laser) deposit energy E at $r=0$. This energy will generate a shock wave which propagates with velocity $V_s(t)$ spherically outward to radius $R_s(t)$. Equations (1) and (2) represent the nonuniform conditions upstream of the shock. The shock velocity relative to the upstream gas is $V_s - u_\ell$. Since u_ℓ is much greater than the upstream speed of sound, the requirement that $V_s > u_\ell$ insures that the shock is strong in the traditional sense of the strong blast wave.[14] The density, pressure, and gas velocity immediately behind the shock become

$$\rho_s(t) = \left(\frac{\gamma+1}{\gamma-1}\right)\rho_l = \left(\frac{\gamma+1}{\gamma-1}\right)^{1/2} \rho^*(r^*)^2 / R_s^{\,2}(t)$$

$$p_s(t) = \left(\frac{2}{\gamma+1}\right)\rho_l V_s^{\,2}(t)$$

$$= \frac{2}{(\gamma+1)}\left(\frac{\gamma-1}{\gamma+1}\right)^{1/2} \rho^*(r^*)^2 V_s^{\,2}(t)/R_s^{\,2}(t)$$

and

$$u_s(t) = \left(\frac{2}{\gamma+1}\right) V_s(t)$$

respectively.

In order to obtain the density, pressure, and velocity everywhere between $r=0$ and $r=R_s(t)$, we must solve the inviscid Euler equations. The conservation of mass, momentum and energy are, respectively:

$$\frac{\partial \rho}{\partial t} + \frac{\partial(\rho u)}{\partial r} + \frac{2\rho u}{r} = 0$$

$$\frac{\partial u}{\partial t} + u\frac{\partial u}{\partial r} + \frac{1}{\rho}\frac{\partial p}{\partial r} = 0 \tag{3}$$

and

$$\frac{\partial(p/\rho^\gamma)}{\partial t} + u\frac{\partial(p/\rho^\gamma)}{\partial r} = 0$$

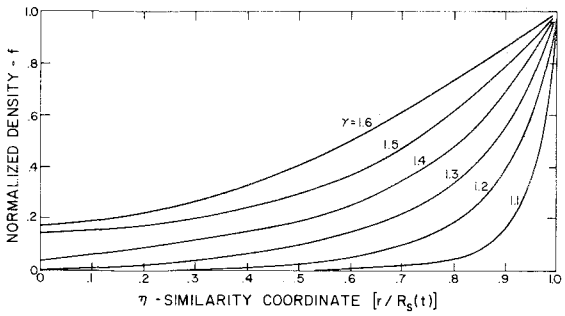

Fig. 2 Density profile behind a strong shock.

We seek a solution to the Euler equations which describes the propagation of a blast wave into a nonuniform gas. Following the traditional solution[14] for a blast wave into a uniform environment, we assume

$$\rho=\rho_s(t)f(\eta) \qquad p=p_s(t)g(\eta)$$

and

$$u=u_s(t)h(\eta)$$

where

$$\eta=r/R_s(t)$$

Substituting the assumed profiles into the Euler equations, we determine the class of solutions for which the variables η and t may be separated. The admissable shock motions are

$$R_s(t)=At^a \tag{4}$$

where A and a are arbitrary constants. The thermal and kinetic energy in the shocked gas must be equal to the energy deposited at $r=0$.

$$E=\int_0^{R_s(t)}(C_vT+\tfrac{1}{2}u^2)\rho\Omega r^2\mathrm{d}r \tag{5}$$

From Eqs. (4) and (5), it follows that

$$a=2/3$$

and

$$A=(E/\rho^*(r^*)^2\Omega I_1)^{1/5} \tag{6}$$

where

$$I_1=\frac{8\int_0^1(g+fh^2)\eta^2\mathrm{d}\eta}{9(\gamma+1)^{3/2}(\gamma-1)^{1/2}} \tag{7}$$

Having separated the η and t variables, we obtain equations for the conservation of mass, momentum and energy, respectively,

$$h'=\left(\frac{\gamma+1}{2}\right)\frac{\eta f'}{f}+(\gamma+1)-\frac{2h}{\eta}-\frac{hf'}{f} \tag{8}$$

$$g'=\frac{1}{2}\left(\frac{\gamma+1}{\gamma-1}\right)hf+\left(\frac{\gamma+1}{\gamma-1}\right)f\left(\eta-\frac{2h}{(\gamma+1)}\right)h' \tag{9}$$

and

$$(\gamma-3/2)(\gamma+1)g+\left(h-\frac{(\gamma+1)\eta}{2}\right)\left(g'-\frac{\gamma gf'}{f}\right)=0 \tag{10}$$

Equations (8) through (10) are integrated from $\eta=1$ to $\eta=0$, subject to the condition that $h(1)=g(1)=f(1)=1$. The density, pressure, and velocity profiles are illustrated in Figs. 2 and 3. Note that the shock profiles are similar to those for a strong blast wave in a uniform atmosphere.[14] The primary difference between the two solutions is that the shock radius in the conical nozzle increases as $t^{2/3}$ whereas the radius of the spherical blast in a uniform atmosphere increases as $t^{2/5}$. The present solution is valid for the time period over which the shock is strong. The limiting time is the time at which the shock velocity decays to the upstream gas velocity. This is denoted by $t_{\max}$ and is determined from

$$V_s(t_{\max})=u_\ell$$

or

$$t_{\max}=\frac{8E\left(\frac{\gamma-1}{\gamma+1}\right)^{3/2}}{27\Omega I_1\rho^*(r^*)^2(u^*)^3} \tag{11}$$

where the integral I_1 is given by Eq. (7) and illustrated in Fig. 4. Additional integral properties of the similarity solution are also illustrated in Fig. 4. The definitions and physical relevance of these quantities will be discussed as the theory is extended to include pulse sequencing.

III. Multiple Pulse Theory

Before extending the fluid mechanical model to include pulse sequencing, we will first define and relate the time average quantities in a notation similar to that used for conventional rockets.

Consider a pulsed laser propulsion system in which mass M is released per cycle and t_p is the time between pulses (in contrast to the pulse duration). The time average mass flux, thrust and power are defined by

$$\bar{\dot{M}}=M/t_p \tag{12}$$

$$\bar{T}=\frac{1}{t_p}\int_0^{t_p}T\mathrm{d}t \tag{13}$$

and

$$\bar{P}=\frac{1}{t_p}\int_0^{t_p}P\mathrm{d}t \tag{14}$$

respectively. The specific impulse, I_{sp}, is defined in terms of the time average thrust and mass flux

$$I_{sp}=\frac{\bar{T}}{\bar{\dot{M}}g} \tag{15}$$

where g is the acceleration of gravity. In addition to the time-average quantities, it is necessary to define a mass average quantity. Denoting the nozzle exit plane velocity of the mass element $\mathrm{d}m$ as u_e, we express the mass average exit plane velocity as

$$\bar{u}_e=\frac{1}{M}\int_0^M u_e\mathrm{d}m \tag{16}$$

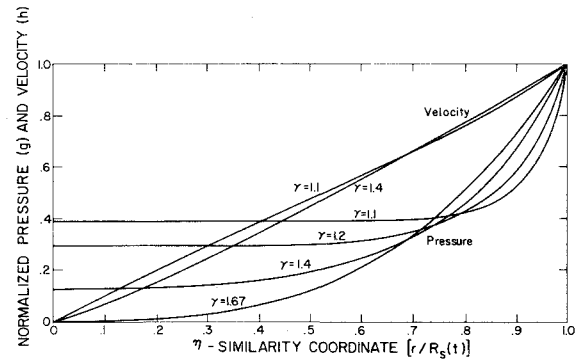

Fig. 3 Pressure and velocity profiles behind a strong shock.

We seek to determine the optimum thrust $\bar{T}$ for the minimum time average laser power $\bar{P}$.† In the limit of zero temperature at the exit plane, the instantaneous thrust T is related to $\bar{u}_e$ by

$$\int_0^{t_p} T\mathrm{d}t = M\bar{u}_e F(\theta_c) \tag{17}$$

where $F(\theta_c)$ represents the loss in the thrust due to the flow divergence at the nozzle exit plane. The instantaneous laser power P is related to the kinetic energy by

$$\int_0^{t_p} P\mathrm{d}t = (1/2)M\bar{u}_e^2 \int_0^1 \left(\frac{u_e}{\bar{u}_e}\right)^2 \mathrm{d}\left(\frac{m}{M}\right) \tag{18}$$

where it has been assumed that all of the laser energy has been converted to fluid kinetic energy. There are no viscous or radiative losses nor is any dissociated gas frozen in the supersonic expansion. From Eqs. (13), (14), (17), and (18), the ratio of thrust to power is expressed as

$$\frac{\bar{T}}{\bar{P}} = \frac{2F(\theta_c)/\bar{u}_e}{\int_0^1 \left(\frac{u_e}{\bar{u}_e}\right)^2 \mathrm{d}\left(\frac{m}{M}\right)} \tag{19}$$

The mass average exit plane velocity is related to the specific impulse via Eqs. (13), (15), and (17).

$$I_{sp} = \bar{u}_e F(\theta_c)/g \tag{20}$$

Eliminating $\bar{u}_e$ between Eqs. (19) and (20), the ratio of thrust to power becomes

$$\frac{\bar{T}}{\bar{P}} = \frac{2F^2(\theta_c)e_R}{gI_{sp}} \tag{21}$$

where e_R is defined as the relative efficiency and is expressed as

$$e_R = \left[\int_0^1 \left(\frac{u_e}{\bar{u}_e}\right)^2 \mathrm{d}\left(\frac{m}{M}\right)\right]^{-1} \tag{22}$$

The quantity e_R is a measure of the energy efficiency of a pulsed device relative to a continuous working (CW) or steady-state device. For CW laser propulsion, the flow is steady and the exit plane velocity is the same for all mass elements. Hence, e_R is identically unity and the CW device is the reference state for the relative efficiency. From the mathematical definition of $\bar{u}_e$, it follows that

$$e_R \leq 1 \tag{23}$$

To understand the physical meaning of the relative efficiency, consider a nozzle from which mass $M/2$ exits with velocity $V+\epsilon$ and mass $M/2$ exists with velocity $V-\epsilon$. The net momentum is MV but the energy required is $\frac{1}{2}M(V^2+\epsilon^2)$. Hence, the thrust to power is reduced with increasing nonuniformity, ϵ. For pulsed laser propulsion, the energy deposition is not uniform and lower efficiencies will result. The fluid mechanical model for pulsed laser propulsion is now extended to include pulse sequencing and the relative efficiency of the pulsed device is assessed.

The single pulse model developed in Sec. II assumes that the source flow is established prior to the energy deposition at $r=0$. The high pressure created by the blast will restrain the source flow until such time that the pressure at $r=0$ drops below the pressure of the sonic orifice. The time at which the point source again allows a finite mass flux is denoted by t_s^*, which, by definition, occurs when

$$p_s(t_s^*)g(0) = p^*$$

or

$$t_s^* = \frac{2}{3}\left(\frac{2\gamma g(0)}{\gamma+1}\right)^{1/2}\left(\frac{\gamma-1}{\gamma+1}\right)^{1/4} r^*/u^* \tag{24}$$

Numerical results for t_s^* are illustrated in Fig. 4 and indicate that t_s^* is significantly shorter than the time required for the gas flow through the throat (r^*/u^*). We may wish to consider a mechanical delay in restarting the point source. Hence, we define t_s as the time at which we mechanically allow the source to restart.

$$t_s \geq t_s^*$$

Once the point source is restarted, the source gas will expand into the relative vacuum created by the tail of the previous blast wave. At some time sufficiently greater than t_s, we wish to create a second pulse. Let us define the critical time (t_c) for the next pulse such that the shock will just propagate through the source gas when the shock itself becomes weak. A schematic diagram is presented in Fig. 5a to illustrate the meaning of t_c. The value of t_c is readily determined by balancing the mass released by the source during the time interval ($t_c - t_s$) with the mass swept out by the spherical

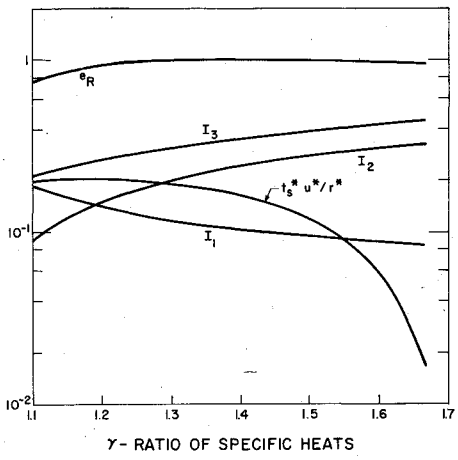

Fig. 4 Integral properties of the similarity solution.

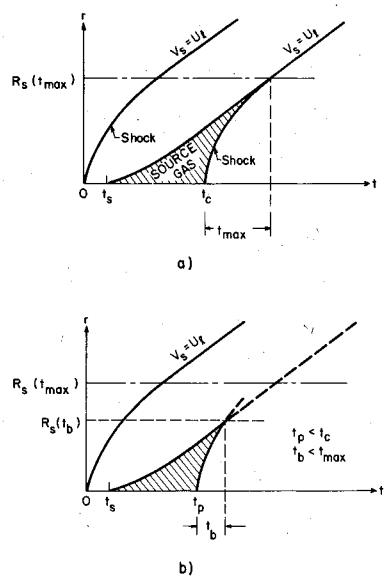

Fig. 5 a) Critical pulse time, t_c; b) shock "breakthrough" time, t_b.

†Note that the time average laser power is the average continuous power delivered by a repetitively pulsed device. The peak laser power is the average power delivered over the duration of the laser pulse. The latter concept is not used in this paper.

shock as it passes through the source gas. Therefore,

$$\rho^* u^* (r^*)^2 \Omega (t_c - t_s) = \int_0^{t_{max}} \rho_l V_s \Omega R_s^2 dt$$

or

$$R_s (t_{max}) = (t_c - t_s) u_l$$

Since t_{max} is defined by $V_s (t_{max}) = u_l$, it follows that

$$t_c - t_s = \frac{3}{2} t_{max} \tag{25}$$

We wish to restrict the time between pulses (t_p) such that

$$t_p \leq t_c \tag{26}$$

otherwise, the shock will become weak before it propagates through all of the source gas and a lower specific impulse will result. For pulse repetition frequencies which satisfy Eq. (26), the shock will "break through" the source gas in a time (after energy deposition) less than t_{max}. Let us denote this time by t_b, as depicted in Fig. 5b. We may evaluate t_b in a manner identical to that used in determining t_c. Mass balance again requires

$$R_s (t_b) = (t_p - t_s) u_l \tag{27}$$

or

$$t_b = ((t_p - t_s) u_l / A)^{3/2} \tag{28}$$

At time t_b (after energy deposition) we have a high pressure gas which must expand isentropically to the exit plane of the rocket nozzle. The gas is located between $r=0$ and $R_s (t_b)$. The gas density, pressure and velocity are, respectively,

$$\rho_b = \rho_s (t_b) f(\eta_b)$$

$$p_b = p_s (t_b) g(\eta_b)$$

and

$$u_b = u_s (t_b) h(\eta_b)$$

where

$$\eta_b = r / R_s (t_b)$$

Each mass element dm,

$$\frac{dm}{M} = \frac{\Omega \rho_s (t_b) R_s^3 (t_b) f(\eta_b) \eta_b^2 d\eta_b}{\rho^* u^* (r^*)^2 \Omega (t_p - t_s)}$$

may expand to the maximum exit plane velocity

$$u_e = u_s (t_b) [h^2 (\eta_b) + \gamma g (\eta_b) / f(\eta_b)]^{1/2} \tag{29}$$

corresponding to zero temperature and pressure. The mass average exit plane velocity, Eq. (16), becomes

$$\bar{u}_e = \frac{2 I_2 u_l}{(\gamma - 1)(\tau)^{1/2}} \tag{30}$$

where

$$\tau = \frac{t_p - t_s}{t_c - t_s}$$

and

$$I_2 = \int_0^1 f \eta^2 (h^2 + \gamma g / f)^{1/2} d\eta \tag{31}$$

where we have noted that the integrals over η_b and η are equivalent. From u_e and $\bar{u}_e$, Eq. (22) is evaluated to determine the relative efficiency

$$e_R = \frac{(\gamma + 1) I_2^2}{(\gamma - 1) I_3} \tag{32}$$

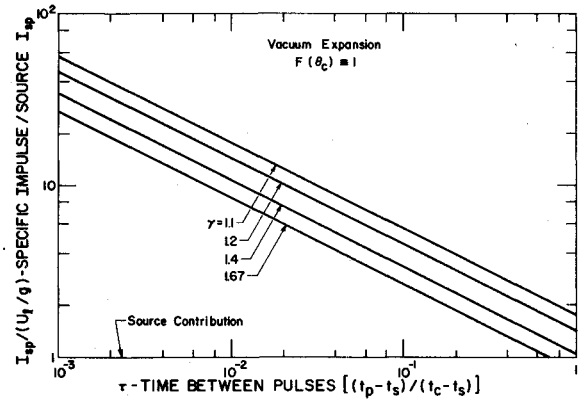

Fig. 6 Enhancement of specific impulse.

where

$$I_3 = \int_0^1 (f h^2 + \gamma g) \eta^2 d\eta \tag{33}$$

Numerical results for I_2, I_3 and e_R are illustrated in Fig. 4. These results indicate that, for all practical purposes, the pulsed laser propulsion system is fluid mechanically as efficient as the CW system. The reason for this result is that the bulk of the mass lies immediately behind the shock where the velocity is approximately the same for all mass elements. Hence, the relative efficiency, as defined by Eq. (22), is nearly unity.

Having shown that the pulsed laser propulsion concept is fluid mechanically as efficient as the CW operation, we now use Eqs. (20) and (30) to determine the specific impulse.

$$\frac{I_{sp}}{(u_l / g)} = \frac{2 I_2 F(\theta_c)}{(\gamma - 1)(\tau)^{1/2}} \tag{34}$$

The specific impulse is normalized to u_l/g, the specific impulse of the source gas without energy addition, and the results are illustrated in Fig. 6. Note that $\tau < 1$ is required in order to obtain a specific impulse significantly greater than that of the source gas alone. This is consistent with the previously imposed constraint that t_p must be less than t_c. Equation (34) also illustrates that the specific impulse becomes unbounded as $\tau \to 0$. This is due to the fact that the time average laser power is also unbounded in this limit. We may rewrite the specific impulse in dimensional form using Eqs. (15) and (21)

$$I_{sp} = \frac{(2 e_R)^{1/2}}{g} \left(\frac{\bar{P}}{\dot{M}} \right)^{1/2} F(\theta_c) \tag{35}$$

where the time average mass flow is defined as

$$\dot{M} = \frac{M}{t_p} = \frac{\dot{M} (t_p - t_s)}{t_p} \tag{36}$$

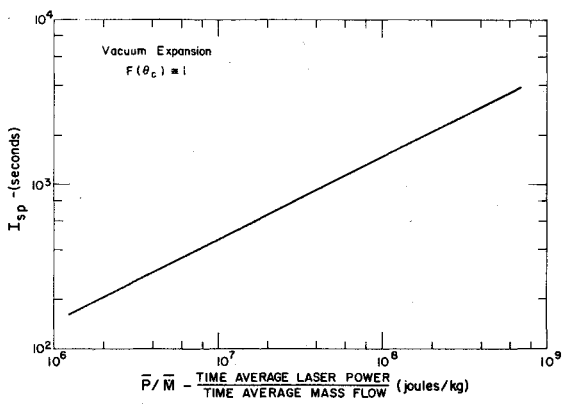

Fig. 7 Specific impulse.

and the time average laser power is

$$\bar{P}=E/t_p \tag{37}$$

The theoretical limit of the specific impulse is illustrated in Fig. 7. The specific impulse is limited only by the amount of energy that can be deposited into a given mass flux and is independent of the pulse repetition frequency.

Since the throat diameter D^* of the rocket nozzle is related to the source radius r^* by continuity,

$$M=\rho^* u^* \Omega (r^*)^2 = \rho^* u^* \pi (D^*)^2/4$$

Eqs. (35) through (37) yield

$$I_{sp}=\frac{1}{g}\left(\frac{8e_R}{\pi}\right)^{1/2}\left(\frac{E}{\rho^* u^* (D^*)^2 (t_p-t_s)}\right)^{1/2} F(\theta_c) \tag{38}$$

which will be our primary working equation when, in Sec. IV, we consider the laser requirements necessary to propel a given system.

It is interesting to note the scaling of the specific impulse with molecular weight. First, we recall that in the chemical rocket, the specific impulse scales in direct proportion to u^*. At constant temperature, the specific impulse scales as the inverse square root of the molecular weight, thereby favoring a low molecular weight propellant. For the case of pulsed laser propulsion, we shall retain both the chamber pressure and the laser power constant. Rewriting Eq. (38) with ρ^* replaced by $\gamma p^*/(u^*)^2$, we obtain

$$I_{sp}=\frac{1}{g}\left(\frac{8e_R}{\pi}\right)^{1/2}\left(\frac{u^* E}{\gamma p^* (D^*)^2 (t_p-t_s)}\right)^{1/2} F(\theta_c) \tag{39}$$

which illustrates that the I_{sp} scales as the square root of u^* and the inverse fourth root of the molecular weight, thereby favoring a low molecular weight propellant, but not by as large a margin as in the chemical rocket.

The results derived above are appropriate only for nozzles exhausting with negligible temperature and pressure. In addition, we have assumed that there is no divergence of the flow at the nozzle exit plane. The loss in thrust due to finite ambient pressure, and that due to the finite size and shape of rocket nozzles, will now be determined in order to demonstrate the operational limitations of pulsed laser propulsion.

IV. Operational Limitations

There are several effects which limit the specific impulse that we may obtain from a pulsed laser propulsion system such as that analyzed in the previous sections. They are: 1) finite divergence of the nozzle, 2) finite length of the nozzle, and 3) finite ambient pressure. These three effects can be included in the present fluid mechanical analysis of pulsed laser propulsion.

In determining the thrust from a pulsed laser propelled rocket, we have assumed, without explicitly stating, that the rocket nozzle is contoured such that the initial conical flow may exhaust from the nozzle without divergence. In the absence of any such contouring, some thrust will be lost due to the divergence of the flow. The effect is easily assessed by determining the mass average of $u_e\cos\theta$, rather than the mass average of u_e. The specific impulse is reduced by the factor $F(\theta_C)$ which is given by

$$F(\theta_C)=\frac{\sin^2\theta_C}{2(1-\cos\theta_C)}$$

where θ_C is the cone half angle and is related to Ω by

$$\Omega=2\pi(1-\cos\theta_C)$$

For cone half angles of 10°, 20° and 30°, the specific impulse is reduced by 1%, 3% and 7%, respectively. Hence, nozzle contouring will be a refinement, rather than a primary fluid mechanical consideration.

The length of the nozzle is restricted by the radius of the shock at "breakthrough." The shock must be contained within the nozzle, otherwise the specific impulse will be reduced. This is expressed as

$$L \geq R_s(t_b) \tag{40}$$

where L is the nozzle length and $R_s(t_b)$ is the shock "breakthrough" radius, given by Eq. (27).

$$R_s(t_b)=\left(\frac{\gamma+1}{\gamma-1}\right)^{1/2}\left(\frac{t_p-t_s}{D^*/u^*}\right)D^* \tag{41}$$

However, satisfying Eq. (40) does not insure that the maximum thrust is obtained from the energy deposition. In order to obtain the results predicted by Eq. (38), the gas must expand to a vacuum while still within the nozzle. To determine the effect of the finite value of L on the I_{sp}, we allow the gas to expand isentropically to the exit plane at $r=L$. To simplify this analysis it is assumed that the unsteady expansion is initially similar to the steady flow in a diverging conical nozzle. Late time oscillations are created by a rarefaction wave returning from the exit plane. These oscillations are neglected in this model since they occur only during the subsonic portion of the expansion, at which time most of the momentum transfer has already occured. We conserve mass, entropy, and energy by

$$\rho_e u_e L^2 = \rho_b u_b \eta_b^2 R_s^2(t_b) \tag{42}$$

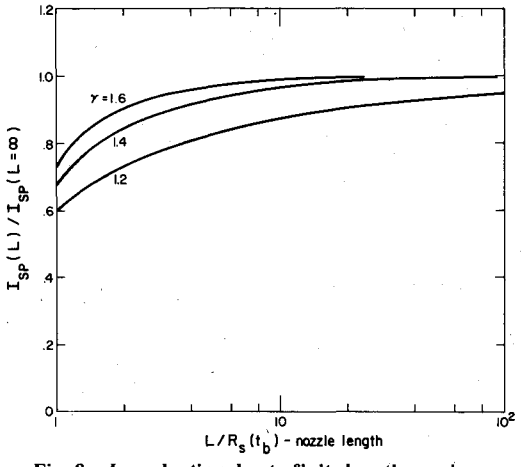

Fig. 8 I_{sp} reduction due to finite length nozzles.

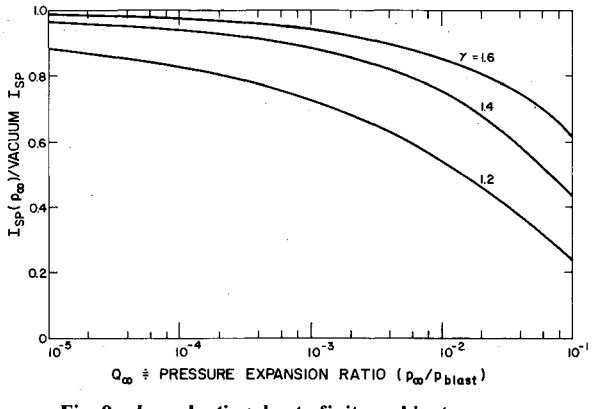

Fig. 9 I_{sp} reduction due to finite ambient pressure.

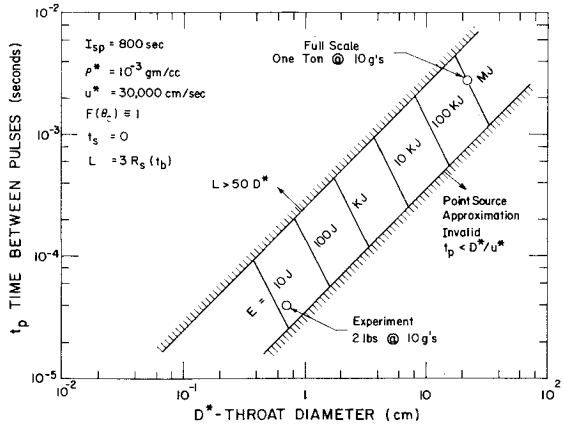

Fig. 10 Laser energy requirements.

$$p_b/\rho_b{}^{\gamma} = p_e/\rho_e{}^{\gamma} \tag{43}$$

and

$$C_p T_e + 1/2 u_e^2 = C_p T_b + 1/2 u_b^2 \tag{44}$$

respectively, where the subscripts b and e denote "breakthrough" and exit plane conditions, respectively. Solving Eqs. (42) through (44) for $u_e(L)$, the reduced specific impulse due to the finite nozzle length is obtained by using the corrected value of u_e in the integrand of I_2. Results are illustrated in Fig. 8. For $\gamma = 1.4$, termination of the nozzle at the breakthrough radius would result in a recovery of only 68% of the I_{sp}. However, 90% of the I_{sp} is recovered in three breakthrough radii. Nozzle lengths greater than three $R_s(t_b)$ yield a diminishing return in terms of the I_{sp} recovered. We shall use $L = 3\,R_s(t_b)$ as a design criterion.

The finite ambient pressure will also reduce the specific impulse of the laser powered rocket. To illustrate the magnitude of this effect, we again allow the gas to expand isentropically from the "breakthrough" conditions to the ambient pressure, p_∞. Conservation of entropy and energy, Eqs. (43) and (44), yield

$$u_e = u_s(t_b)\,[h^2(\eta_b) + \gamma g(\eta_b)/f(\eta_b) - \Gamma(\eta_b)]^{1/2}$$

where

$$\Gamma(\eta_b) = \gamma \left[\frac{9(\gamma+1)^3}{8(\gamma-1)^2} I_1 Q_\infty\right]^{\frac{\gamma-1}{\gamma}} g^{\frac{1}{\gamma}}(\eta_b)/f(\eta_b)$$

and

$$Q_\infty = \Omega P_\infty (u^*)^3 (t_p - t_s)^3/E$$

where Q_∞ is approximately the ratio of p_∞ to the pressure of the blast wave.

The reduced specific impulse due to the finite ambient pressure is obtained by using the corrected value of u_e in the integrand of I_2. Results are illustrated in Fig. 9. For a chamber pressure of two atmospheres (sufficient to "choke" the flow at sea level), the sonic pressure is one atm. Laser energies sufficient to create a 30,000K plasma would result in a blast wave pressure of 100 atm. Thus, the sea level value of Q_∞ would be 10^{-2} and, for $\gamma = 1.4$, 75% of the vacuum I_{sp} would be obtained. Raising the chamber pressure to 20 atm would result in a 1000 atm blast wave and a recovery of 90% of the vacuum I_{sp}. Higher chamber pressures yield a diminishing return in the I_{sp} recovered and would begin to introduce structural penalties, as well as thermodynamic losses due to the compression of the propellant.

Having determined the limitations for which the vacuum results are valid, we will illustrate these results by way of a simple example. From Eq. (21), we recall the relation between power $\bar{P}$ and thrust $\bar{T}$

$$\bar{P} = g I_{sp} \bar{T}/2F^2(\theta_c) e_R \tag{45}$$

where

$$\bar{P} = E/t_p \tag{46}$$

Equations (38) and (45) yield the size of a rocket required for the thrust $\bar{T}$.

$$D^* = \frac{2}{(\rho^* u^* \pi g I_{sp})^{1/2}} \left(\frac{t_p}{t_p - t_s}\right)^{1/2} (\bar{T})^{1/2} \tag{47}$$

If we wish to design a rocket to operate with a chamber pressure of two atm and temperature of 300K, the sonic density and velocity become 10^{-3} gm/cc and 30,000 cm/sec, respectively. Let us consider launching a one ton rocket with 10 g's acceleration and a specific impulse of 800 sec. This requires an orifice diameter of 22 cm and a power of 350 MW. In a laboratory experiment, we may consider an equivalent acceleration of a 2 pound rocket which requires $D^* = 7$ mm and $\bar{P} = 0.35$ MW. The remaining point to illustrate is that there are distinct combinations of E and t_p permitted by the nozzle fluid mechanics. These are illustrated in Fig. 10 where we illustrate, from Eq. (38), t_p vs D^* at constant E. For arbitrary values of the orifice diameter, D^*, there is a lower limit on the time between pulses for which the point source approximation is valid. This reflects the fact that a finite time is required for the source gas to enter the rocket nozzle. There also exists an upper limit on the time between pulses for which a nozzle of a given length can recover the optimum thrust from the energy deposited. Larger time durations between pulses would permit the source gas to escape the nozzle before all of the pressure were converted to momentum. Our design criterion required that the nozzle length be three "breakthrough" radii to recover 90% of the specific impulse. Nozzle lengths greater than 50 D^* are excluded on the basis of their large aspect ratio. The illustrative examples indicate that the laboratory experiment could be conducted with a 15 joule laser operating at 25,000 pulses per second. Launching one ton with 20,000 lb_f of thrust would require a megajoule laser operating at 350 pulses per second.

V. Summary and Conclusions

A fluid mechanical model has been developed to describe the flow within a conical nozzle that is subjected to point energy depositions at the apex of the cone. The model has been used to assess the concept of pulsed laser propulsion.[4] The specific impulse of a pulsed laser propelled rocket has been obtained as a function of nozzle sonic conditions, the laser energy and the pulse repetition frequency. The results are given by Eq. (38) and illustrated in Fig. 10. Large specific impulses may be obtained with moderate energy densities and pulse repetition frequencies. However, these results are valid only for an expansion to a vacuum. The reduction in the thrust due to a finite exit plane pressure may be significant. The finite exit plane pressure may arise due to either the finite ambient pressure, or the finite length of the rocket nozzle. The degradation of the specific impulse due to both of these effects has been assessed.

The relative efficiency of a pulsed propulsion system has been defined and determined. This efficiency is based on fluid mechanical considerations only, and the laser absorption mechanisms have not been considered. That is, we have assumed, for both CW and pulsed, that all of the laser energy has been absorbed by the working medium. Results indicate that pulsed laser propulsion is approximately 98% to 99% as efficient as the CW device in converting laser power to thrust. Hence, pulsed laser propulsion appears as versatile and as efficient as the CW technique. However, pulsed laser propulsion has the potential advantages of simplicity in engine design and the elimination of possible plasma stability

constraints that may be associated with CW laser propulsion systems.

Acknowledgment

This research was supported by the Advanced Research Projects Agency of the Department of Defense and was monitored by Office of Naval Research under Contract No. N00014-76-C-0738.

References

[1]Kantrowitz, A. R., "Propulsion to Orbit by Ground-Based Lasers," *Astronautics and Aeronautics*, Vol. 10, May 1972, p. 74.

[2]Pirri, A. N. and Weiss, R. F., "Laser Propulsion," AIAA Paper 72-719, Boston, Mass., 1972.

[3]Rom, F. E. and Putre, H. A., "Laser Propulsion," NASA TM-X-2510, April 1972.

[4]Pirri, A. N., Monsler, M. J., and Nebolsine, P. E., "Propulsion by Absorption of Laser Radiation," *AIAA Journal*, Vol. 12, Sept. 1974, pp. 1254-1261.

[5]Papailiou, D. D., ed., "Frontiers in Propulsion Research: Laser, Matter—Antimatter, Excited Helium, Energy Exchange, Thermonuclear Fusion," Jet Propulsion Laboratory, Pasadena, Calif., NASA TM 33-722, March 1975.

[6]Myrabo, L. N., "MHD Propulsion by Absorption of Laser Radiation," *Journal of Spacecraft and Rockets*, Vol. 13, Aug. 1976, pp. 466-472.

[7]Caledonia, G. E., Wu, P. K. S., and Pirri, A. N., "Radiant Energy Absorption Studies for Laser Propulsion," NASA Report CR-134809, Physical Sciences Inc. Report TR-20, March 1975; also P. K. S. Wu and Pirri, A. N., "Stability of Laser Heated Flows," *AIAA Journal*, Vol. 14, March 1976, pp. 390-392.

[8]Pirri, A. N., Schlier, R., and Northam, D., "Momentum Transfer and Plasma Formation above a Surface with a High Power CO_2 Laser," *Applied Physics Letters*, Vol. 21, Aug. 1972, pp. 79-81.

[9]Lowder, J. E., Lencioni, D. E., Hilton, T. W., and Hull, R. J., "High-Energy Pulsed CO_2 Laser-Target Interaction in Air," *Journal of Applied Physics*, Vol. 44, June 1973, p. 2759.

[10]Pirri, A. N., "Theory for Momentum Transfer to a Surface with a High-Power Laser," *The Physics of Fluids*, Vol. 16, Sept. 1973, p. 1435.

[11]Hall, R. B., Maher, W. E., and Wei, P. S. P., "An Investigation of Laser-Supported Detonation Waves," Air Force Weapons Lab., Kirtland AFB, N. Mex., AFWL-TR-73-28, June 1973.

[12]Hettche, L. R., Schriempf, J. T., and Stegman, R. L., "Impulse Reaction Resulting from the In-Air Irradiation of Aluminum by a Pulsed CO_2 Laser," *Journal of Applied Physics*, Vol. 44, Sept. 1973, p. 4079.

[13]Back, L. H. and Varsi, G., "Detonation Propulsion for High Pressure Environments," *AIAA Journal*, Vol. 12, Aug. 1974, pp. 1123-1130.

[14]Sedov, L. I., *Similarity and Dimensional Methods in Mechanics*, (M. Holt, ed.), Academic Press, New York, 1959.